

# Fast genomic optical map assembly algorithm using binary representation

Przemysław Stawczyk and Robert Nowak  
Institute of Computer Science, Warsaw University of Technology,  
Warsaw, Poland

2022.10.12

1

## Abstract

Reducing the cost of sequencing genomes provided by next-generation sequencing technologies has greatly increased the number of genomic projects. As a result, there is a growing need for better assembly and assembly validation methods. One promising idea is to use heterogeneous data in assembly projects. Optical Mapping (OM) is beneficial in validating genomic assemblies, correction and scaffolding. Single raw OM read describes a DNA molecule's long fragment, up to 1Mbp. Raw OM data from the same genome could be assembled to create consensus maps that span an entire chromosome. The assembly process is computationally hard because of the large number of errors in input data. This work describes a new algorithm and computer program to assemble OM reads without a reference genome. In our algorithm, we explored binary representation for genome maps. We focused on the efficiency of data structures and algorithms and scale on parallel platforms. The algorithm consists of several steps, of which the most important are : (1) conversion of the restriction maps into binary strings, (2) detection of overlaps between restriction maps, (3) determining the layout of restriction maps set, (4) creation of consensus genomic maps. Our algorithm deals with optical mapping data with low error levels but fails with high-level error reads. We developed a software library, console application and module for Python language. The approach presented in this paper proved to be faster than a dynamic programming approach and performed well on error-free data. It could be used as a step of *de novo* assembly pipelines or to detect misassemblies. The software is freely available in a public repository under GNU LGPL v3 license (<https://sourceforge.net/p/binary-genome-maps/code>).

**Keywords:** optical mapping; genome mapping; consensus; next generation sequencing.

---

<sup>1</sup>Further author information: (Send correspondence to Robert Nowak) Robert Nowak: Tel: +48 22 2347718; E-mail: robert.nowak@pw.edu.pl

# 1 Introduction

Reducing the cost of sequencing genomes has greatly increased the number of genomic projects and raw read data available. Better sequencing results have been enabled by better software for assembly and scaffolding. More efficient algorithms can properly use the increasing volume of available data. With data from different sequencing technologies, Heterogeneous sequencing is an effective method of improving sequencing results. We propose that optical mapping results be included in heterogeneous sequencing.

Optical Mapping (OM) has been found to be very useful in structural variation analysis, validating genomic assemblies [21], correction and scaffolding assembled contigs [4, 6]. In the OM process, DNA is first isolated before nicking enzymes are used to digest DNA strands [25]. The digested DNA is later imaged [20] to determine the distances between the labels on a DNA strand. The process generates information about the placement of label sites on DNA strands, referred to as restriction maps (rmaps). Rmaps are analogous to sequence reads in the context of genome sequencing and have a length of 150Kbp – 1.6Mbp [18]. Rmaps can be assembled to create consensus maps. The result of such an assembly can cover an entire chromosome. Some of the best-known companies currently developing OM methods are Bionano Genomics [1] and Nabsys [15].

Other than proprietary software from sequencer manufacturers, few algorithms for creating whole-genome maps have been developed. Past projects have been based upon dynamic programming with backtracking [11] which scales very poorly with larger genomes, such as the human genome. Newer algorithms have been developed only for resequencing assembly projects, as they require reference map [9, 12].

In our new algorithm, we explore the possibility of using different genome map representations by binary strings. Although this algorithm is more sensitive to incorrect indexes of marker positions, it could be used in *de novo* assemblies, as it does not require a reference genome or reference maps. Our assembly algorithms could be executed on high-parallel platforms – we have focused on efficiency and the ability to scale with parallel execution. The software library and application were developed in C++ and are freely available as open-source.

# 2 Materials and methods

Our assembly algorithm is based on an overlap-layout-consensus model. It uses a binary representation of genomic maps, enabling efficient computational resources. Short binary sequences can be easily compared using an XOR operation directly implemented in every modern processor. The algorithm consists of four steps:

- Converting rmaps to binary string.
- Overlap detection – scoring the similarities of each pair of rmaps.
- Layout forming – resolving conflicts in neighbouring rmaps.
- Consensus – constructing the contiguous output.

The algorithm steps are described below.

## Genomic map representation

A restriction map (rmap) is a set of marker positions relative to a genome fragment. A consensus genome map is created during assembly from rmaps for the same genome or chromosome. The representation of a consensus genome map and a single restriction map is similar. It is an ordered set of marker positions relative to the beginning of a genome fragment or chromosome. We propose a new representation based on quantization and binary sequences. Each position in a binary sequence represents a constant genome fragment called a quant, the length of each quant is the same. '1' in the sequence indicates at least one marker present in the quant, while '0' indicates no markers. We depict such a representation in Figure 1.

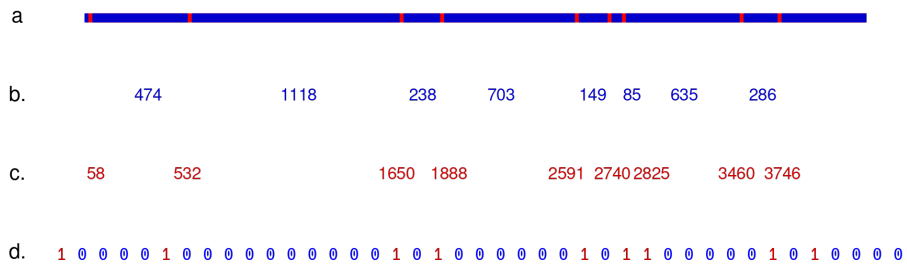


Figure 1: Genomic map representations (example for a genome of size 4000). a.– genome with markers marked in red, b. – distances between markers, c. – marker positions, d. – binary map for quant size = 100.

Converting a rmap into a binary string leads to a loss of information, namely, the exact relative positions of the markers. We call this issue a quantization error. Rmaps from the same genome fragment quantized with the same quant length can produce different binary string representations. The different placement of quant borders results in the relative placement of markers in binary sequence representations. Moreover, two markers close to each other can be represented as one bit or two neighbour bits. We present a simple example of such differences in Figure 2. These effects are less pronounced with low marker density but must be accounted for in an algorithm.

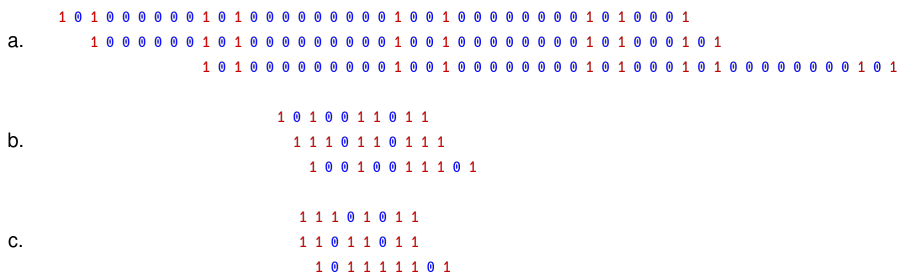


Figure 2: Quantization errors visualization. a. – aligned maps from the same genome fragment, b. – aligned maps from a. quantized with quant length 4, c. – aligned maps from a. quantized with quant length 5.



---

**Algorithm 1** Overlap search for left neighbor

---

```
1: function FINDLEFTALIGNMENT(ref, aligned)
2:    $maxShift \leftarrow \text{MINLEN}(ref, aligned)$ 
    $\triangleright$  could be adjusted to be e.g. half of smaller rmap
3:    $bestAlign \leftarrow 1$ 
    $\triangleright$  differentiating part, 1 means that all bits differ, 0 means full conformance.
4:    $bestShift \leftarrow 0$ 
    $\triangleright$  shift between rmaps ends
5:   for  $shift \in \{1, \dots, maxShift\}$  do
6:      $test \leftarrow aligned \ll shift$ 
7:      $result \leftarrow test \text{ XOR } ref$ 
8:     TRUNCATELONGER( $test, ref$ )
9:     if  $\text{COUNT}(result) / \text{LEN}(result) < bestAlign$  then
    $\triangleright$  it's a better alignment
10:       $bestAlign \leftarrow \text{COUNT}(result) / \text{LEN}(result)$ 
11:       $bestShift \leftarrow shift$ 
   return  $bestShift$ 
```

---

computation time too much. Our algorithm has a parameter that allows the end-user to set another value. We commonly set this value to 20%, or even 30% in numerical experiments, also allowing less precise alignments.

Our method for layout determination is presented as Algorithm 2.

---

**Algorithm 2** Global rmaps alignment

---

```
1: procedure FINDGLOBALALIGNMENT(rmaps)
2:   for  $i \in \{0, 1 \dots \text{LEN}(rmaps)\}$  do
3:      $smallestShift \leftarrow \text{LEN}(rmaps[i])$ 
4:      $leftRMap \leftarrow i$ 
5:     for  $j \in \{0, 1 \dots \text{LEN}(rmaps)\}$  do
6:       if  $i == j$  then
7:         continue
8:        $result \leftarrow \text{FINDLEFTALIGNMENT}(rmaps[i], rmaps[j])$ 
9:       if  $smallestShift > result$  then
10:         $smallestShift \leftarrow result$ 
11:         $leftRMap \leftarrow j$ 
12:      $rmaps[i].addLeftNeighbor(leftRMap)$ 
```

---

After rmaps are detected as neighbours we prepare them for alignment. We eliminate rmaps containing themselves entirely in others. We present a visualization of rmaps layouts in Figure 4.

## Consensus map creation

Contiguous sequences of neighbour rmaps are constructed after aligning all the maps. For contigs detection, we interrogate the graph, where rmaps are the vertex, and the similarity score is the edge. If several vertices form a line, these vertices are traversed using a consensus algorithm. If several vertices form a circle on a graph, the circle is broken.

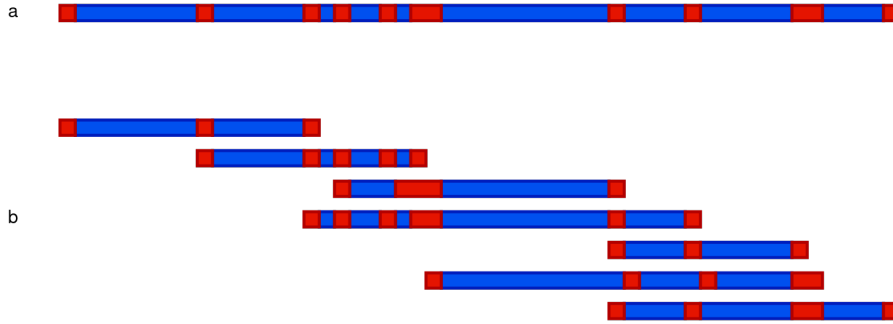


Figure 4: Visualization of aligned rmaps. Red indicates marker in map, blue indicates no marker. a. – reference map, b. – set of aligned rmaps.

Each sequence of rmaps is traversed using a consensus algorithm to create a contiguous map representation. For each position on the aligned rmaps, the number of '1' and '0' are counted, then the most frequent symbol is chosen. In the case of an equal number of '1' and '0', the symbol '1' is chosen because the rmap representation is sparse and losing information about a marker is considered a more significant issue than adding a non-existing marker. We present this process in Algorithm 3.

---

**Algorithm 3** Consensus algorithm

---

```

1: function PERFORMCONSENSUS(contig)
2:   map  $\leftarrow$  []
3:   count  $\leftarrow$  0
4:   for  $p \in \{0, 1, \dots, \text{LEN}(\text{contig}) - 1\}$  do
        $\triangleright$   $p$  - position from beginning of overlapping maps
5:     for  $rmap \in \text{MAPSATPOS}(\text{contig}, p)$  do
6:       if  $rmap.at(p) == 1$  then  $\triangleright$   $rmap.at(p)$  - value on position  $p$ 
7:         count  $\leftarrow$  count + 1
8:       if count < ( $k/2$ ) then
9:         map.append(0)
10:      else
11:        map.append(1)
   return map

```

---

### Assembly parameters

Our application allows users to adjust certain parameters of the assembly:

- *margin quant* – the minimal length of overlap (i. e., common fragment of rmaps pair) in quants.
- *margin part* – minimal part of the smaller map to consider for overlap (i. e. if the margin is 0.25, the overlap has to be at least 25% of smaller map length in size)

- *threshold* – the threshold of differences to consider an overlap meaningful (i. e. if the threshold is 0.15, overlaps with more than 15% of differences on the common part are discarded)
- *marker preference* – consensus preference, symbol to be used in resulting contig if there are 50% of both '0' and '1'
- *folds* – how many times assembly step has to be performed before giving output.

Users can also adjust input and output filenames and the number of threads used. BGM is open source, and the assembly process is modular. For example, further adjustments can be made by changing the cost function in the source code.

### 3 Results

We performed numerical experiments on simulated and real datasets. We compared our approach with an algorithm based on dynamic programming with backtracking. Moreover, we analyzed the computational complexity of our new algorithm. In our experiments we used data from three organisms : *Escherichia coli* [5], *Caenorhabditis elegans* [2], and *Acinetobacter baumannii* [10]. We provide a brief genome sizes summary of the species used in Table 1.

Table 1: Summary of genome sizes and chromosomes count.

species	chromosomes	length [Mbp]
<i>E. coli</i>	1	4.6
<i>C. elegans</i>	7	100.2
<i>A. baumannii</i>	1	3.8

#### Simulated data

We simulated error-free rmaps using a reference genome. The rmaps length was sampled with the normal distribution of a given mean and standard deviation, and the rmaps position was sampled using a uniform distribution. Marker positions were then calculated, with fragments on the ends bearing no markers being removed. Finally, the rmap was quantized with a given quant value (1000 bp in our case). An example of a simulated dataset aligned to a reference genome is presented in Figure 5.

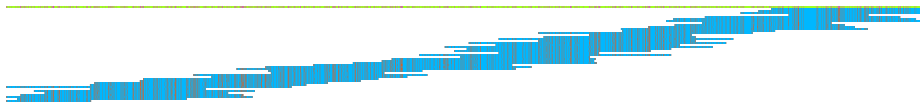


Figure 5: Visualization of simulated rmaps dataset aligned to a reference genome. The reference genome is marked in green, the rmaps in blue and markers are denoted with red. Rmaps come from the *E. coli* genome for the BspQI enzyme and  $15\times$  coverage.

Using simulated datasets from the *E. coli* genome [5] we reconstructed the whole genome consensus map, with simulated BspQI marker and  $7.5\times$  coverage of the genome. For BssSI markers we reconstructed the whole genome for  $10\times$  coverage. Both datasets are summarized in Table 2.

Table 2: Input data that enabled reconstruction of a whole *E. coli* reference map.

enzyme	coverage	rmap count	avg length [Kbp]
BspQI	7.5	36	959.30
BssSI	10	47	1093.00

The the experiment result is visualized in Figure 6.

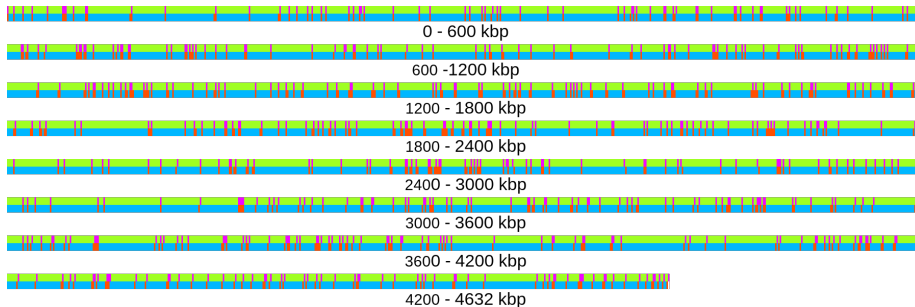


Figure 6: Visualization of assembly results for simulated *E. coli* dataset for BspQI simulated enzyme with  $7.5\times$  coverage. Reference genome is marked in green, result in blue and markers are denoted by red.

## Tuning cost function for overlapping

We analyzed the best overlap using two different cost functions:

1. Number of differences on the overlapping fragment.
2. Differentiating level calculated as the number of differences divided by overlap length.

For comparison, we generated four datasets. Rmap length was sampled from a normal distribution with an expected value of 1 Mbp and a standard deviation of 300 Kbp. The datasets statistics are summarized in Table 3. We only changed the cost function during our experiments, leaving the remaining parameters unaltered. The parameters used in this experiment were : *margin\_part* = 0.5, *margin\_quant* = 100, *folds* = 2, *thresh* = 0.1. The comparison was run on simulated datasets from *E. coli* [5] and *C. elegans* [2] reference genomes. The results of our experiments are also summarized and presented in Table 4.

All rmaps were aligned with at least one other. After analyzing the results, we found that the second function, when the cost was calculated as the number of differences divided by the overlap length, allowed us to connect rmaps more effectively. We decided to use this function in further experiments.

Table 3: Input data for cost function experiments

genome	enzyme	coverage	rmap count	avg. rmap length [Kbp]
<i>E. coli</i>	BspQI	10	47	983.38
<i>E. coli</i>	BspQI	20	92	1003.08
<i>C. elegans</i>	BssSI	10	967	1031.72
<i>C. elegans</i>	BssSI	40	3943	1008.60

Table 4: Results of cost function experiments

function	dataset	contigs count	avg. length [Kbp]	N50 [Kbp]	longest contig [Kbp]
1	<i>E. coli</i> , BspQI 10x	2	3167	4212	4212
2	<i>E. coli</i> , BspQI 10x	2	3387	4633	4633
1	<i>E. coli</i> , BspQI 20x	3	2748	4633	4633
2	<i>E. coli</i> , BspQI 20x	3	2497	4633	4633
1	<i>C. elegans</i> , BssSI 10x	79	2982	2413	8436
2	<i>C. elegans</i> , BssSI 10x	80	3056	2375	7242
1	<i>C. elegans</i> , BssSI 40x	38	11984	5263	17718
2	<i>C. elegans</i> , BssSI 40x	41	11221	4985	20769

## Comparing results of our algorithm with dynamic programming approach

We compared our algorithm to a dynamic programming approach with backtracking [22, 23]. We ran both algorithms on a single thread for comparison purposes, and parameters were unchanged for all runs. We used a server with a Xeon E5-2637 v2 processor (2 cores 4 threads, 3.5 GHz [7]). The comparison was run on simulated datasets from *E. coli* [5] and *C. elegans* [2] reference genomes. We compared performance and quality, measured as run times and the number of contigs. We ran software with a dynamic programming approach developed by *Valouev et al* [24].

Figure 7 summarizes the contigs produced by both algorithms on the *E. coli* dataset. We assume rmaps without gaps cover the input genome (Lander-Waterman theory [8] for genomes used, coverages and rmap sizes). Therefore, we measure the quality of alignment as a number of contigs. The smaller the number of contigs, the better.

The dynamic programming approach needed twice as much coverage to produce a contig with BspQI than our approach did. When simulating BssSI markers, our algorithm reconstructed the whole genome map with 10× coverage, whereas the dynamic programming approach did not produce any contig at all, even with 40× coverage. Due to this, we simulated only the BspQI enzyme when comparing algorithms on the *C. elegans* genome [2]. A summary of the contigs counts during our experiments with the simulated *C. elegans* dataset is presented in Figure 7.

Our experiments show that an algorithm based on binary strings can reconstruct a whole genome with less coverage. The parameters need to be tuned to a specific dataset for best results.

We measured the time needed for both algorithms to finish the assembly. The results are summarized in Figure 8. From all runs, we can see that our

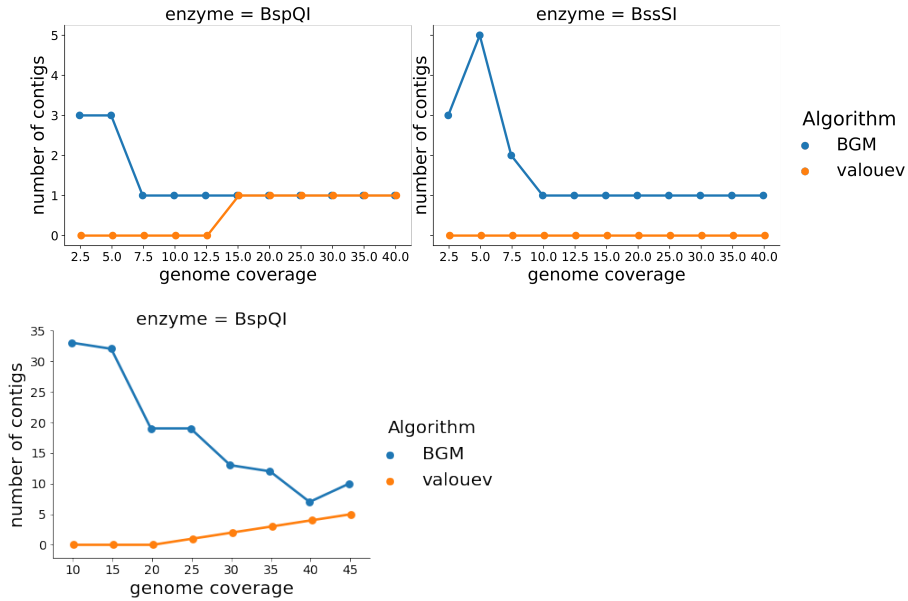


Figure 7: Comparison of contigs count depending on coverage of the genome, *E. coli* dataset (on top), *C. elegans* dataset (on bottom).

approach delivered results around 80 times faster than the dynamic approach on the datasets tested. The complexity of both algorithms is  $\Omega(n^2)$  because each rmap must be analyzed individually, and in both cases, the algorithm must seek an overlap with another rmap.

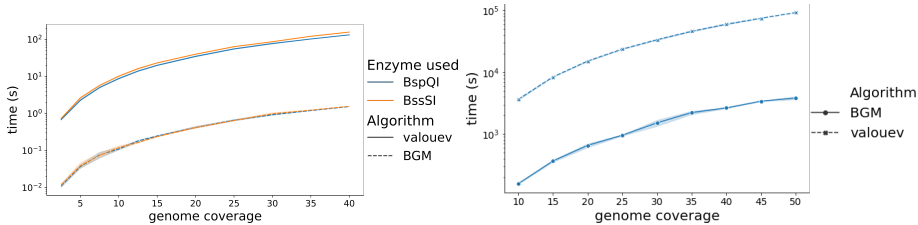


Figure 8: Comparison of time needed for algorithms to finish assembly depending on genome coverage of *E. coli* dataset (on left), and *C. elegans* dataset (on right).

### 3.1 Experiments with exponential rmaps length distribution

We performed an additional experiment using datasets where length was generated using exponential distribution with parameter  $\beta = 150kbp^2$ . Maps shorter

<sup>2</sup> $\beta$  is the scale parameter, which is the inverse of the rate parameter  $\beta = 1/\lambda$ . The rate parameter is an alternative, widely used parameterization of the exponential distribution.

than 100 kbp were discarded, resulting in 275 kbp average length of an rmap. Datasets used were summarized in Table 5.

Table 5: Summary of exponential length datasets

enzyme	coverage	map count	avg. length [kbp]
BssSI	10	173	258.73
BssSI	20	320	279.92
BssSI	30	484	277.45
BssSI	40	651	274.58
BssSI	60	965	277.94
BspQI	10	170	261.48
BspQI	20	316	281.67
BspQI	30	480	277.30
BspQI	40	643	276.26
BspQI	60	957	278.38

We were able to reconstruct the whole *E. coli* genome map using  $30\times$  coverage, both with BspQI and BssSI enzymes simulation. We obtained whole genome maps using parameters :  $margin\_part = 0.3$ ,  $margin\_quant = 90$ ,  $thresh = 0.1$ . BspQI dataset required *folds* parameter to be set on 3 or more, where with BssSI 2 was enough. The dynamic programming approach was able to reconstruct the genome only with  $60\times$  coverage and BspQI enzyme. There was also a partial contig reconstructed with  $60\times$  coverage and BssSI enzyme. Apart from that, the dynamic programming approach produced no contigs.

## Experiments with real data

We performed experiments using a real dataset from the optical mapping of the *A. baumannii* genome [10]. Rmaps from this dataset were converted into binary form using segment lengths of 1000 bp and 1500 bp. We used the entire dataset and subset containing only maps longer than 300 Kbp in both cases. A summary of the datasets is presented in Table 6.

We could not create a consensus map with these datasets, despite changing the parameters. For analysis, we used results from the original genomic project [10] because the authors did not provide the information about the enzyme used. The statistics of the two experiments on filtered datasets are presented in Table 7.

Table 6: Summary of real datasets from *A. baumannii* used in experiments.

dataset	rmap count	avg rmap length [Kbp]
all	51389	214.67
rmapy longer than 300 Kbp	7359	385.20

Even though the dataset has around  $725\times$  genome coverage, we could not create valid contigs. During the experiments, we encountered two anomalies that frequently occurred on the resulting contigs. Some of the maps had long areas free from any markers not present on the reference map. An example of such a contig is presented in Figure 9. The other anomaly in the results was a

Table 7: Summary of experiments with real dataset from *A. baumannii*.

margin_part	margin_quant	thresh	folds	contigs count	N50 [Kbp]	avg contig length [Kbp]
0.5	65	0.08	2	784	395	409.41
0.7	65	0.065	1	1176	408	426.99

significant increase in error frequency the longer the distance from the correct fragment. An example of such an effect is presented in Figure 10.

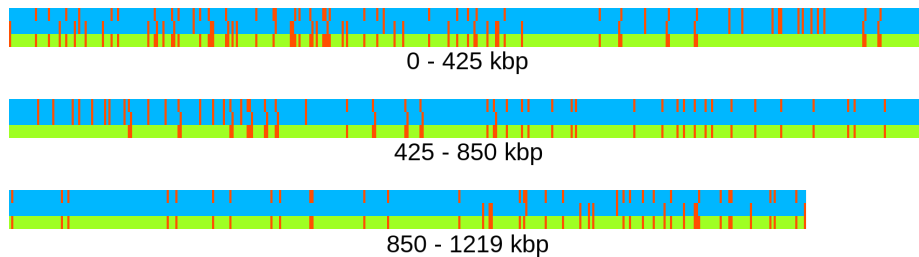


Figure 9: Example of contig with empty space in centre. The reference map and contig are presented in blue with red markers. The reference map is at the top, the contig in the middle. The last row is a comparison where red signifies difference and green signifies conformity.

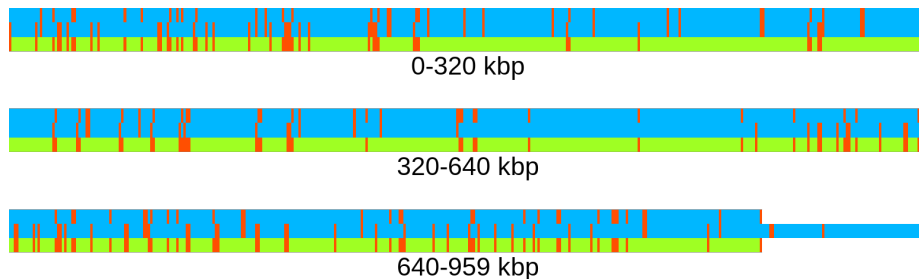


Figure 10: Example of contig with errors at its ends. The reference map and contig are presented in blue with red markers. The reference map is at the top and the contig in the middle. The last row is a comparison where red signifies difference and green signifies conformity.

We assume that most errors were caused by sizing errors and different stretch factors of the molecules scanned. Our algorithm did not address such errors due to the nature of binary sequences.

### Experiment on simulated *A. baumannii*

We performed experiments using a simulated dataset from the same species to check if the genome sequences were not the source of the problems encountered during our experiments with real datasets. We used the reference genome of the

bacteria[3] and generated rmaps datasets simulating nicking of BspQI and BssSI enzymes. The length was sampled from a normal distribution with an expected value of 400 Kbp and a standard deviation of 150 Kbp to match map lengths from a filtered real dataset. We summarize the datasets created in Table 8. For parameters  $margin\_part = 0.3$ ,  $margin\_quant = 105$ ,  $folds = 2$ ,  $thresh = 0.19$ . For rmaps generated simulating the BspQI enzyme we were able to obtain a consensus map covering the whole genome. For rmaps generated using the enzyme, greater sequencing coverage was necessary, and the  $folds$  parameter BssSI was increased to 3. We were also able to create whole-genome consensus maps using datasets with higher (i. e.  $40 - 70\times$ ) genome coverage.

Table 8: Summary of simulated datasets from *A. baumannii* used in experiments.

enzyme	coverage	rmaps count	average length [Kbp]
BspQI	25	244	391.53
BssSI	25	244	397.07

## 4 Discussion

In our experiments, we were able to reconstruct the genomes of *E. coli* and *C. elegans* from simulated error-free datasets. Our algorithm proved faster than a dynamic programming approach and produced results with less genome coverage needed. We used two different enzymes BspQI and BssSI to show that algorithm results are similar for both cases. Our algorithm should work correctly for any enzyme if the sites are spread over the genome.

Our approach can deal with quantization artefacts and the inaccuracy of single-site placement. BGM can also deal with OM errors like false and missing sites, which are present in a binary string as a flipped bit '1' instead of '0' and '0' instead of '1', respectively. Our algorithms deal with dose mistakes and artefacts by allowing differences between rmap alignments. When noise is more significant than a threshold (this is an algorithm parameter set by the user), two noisy rmaps will not be connected. However, due to the nature of binary strings, this approach cannot deal with other kinds of errors, resulting in insertion, deletion, or shift in a binary string. Examples of such errors are stretch variance, sizing errors and missing fragments.

BGM creates a consensus restriction map on chromosome length and could be used to find structural rearrangements. Moreover, BGM can be used as a hybrid de novo assembly step. As presented in our previous work [16] a simultaneous use of available sequencing technologies is useful in improving genome assemblies. BGM algorithm deals with optical mapping data with low error level, e.g. provided by nabsys [17].

With real datasets, our algorithm struggled to produce valid sequences. In our opinion, this effect is due to sizing errors present in the optical mapping data. Even a slightly stretched map of the same fragment of the genome could not be aligned perfectly.

Our approach could be modified and used to align contigs on consensus maps as both contigs and consensus maps have a low error rate. Another option is to use correction algorithms [14, 19] focused on resolving to size and stretch errors

as a part of the assembly pipeline. BGM is fully open source and available at <https://sourceforge.net/projects/binary-genome-maps/>. We would be grateful if someone could adopt any correction algorithm or create a new one. We also share all of the datasets mentioned and encourage the community to perform experiments using our software. We are open to all contributions to our project.

## 5 Conclusion

As more genome mapping and heterogeneous genomic projects are created, it is crucial to develop open-source algorithms to deal with such data. To this end, our paper presents an algorithm based on binary representation to create consensus maps from rmaps. However, judging from the results of the experiments, this algorithm is, in our opinion, better suited for applications with error-free maps like contigs alignment.

## Availability and requirements

BGM is implemented in C++, and is freely available under GNU Library or Lesser General Public License version 3.0 (LGPLv3). It and related materials (like all datasets used) can be downloaded from project homepage <https://sourceforge.net/projects/binary-genome-maps/>.

## Competing interests

The author declares that he has no competing interests.

## Author contributions

PS and RN Identified the problem and designed the approach., PS Implemented the software, worked on testing and validation. PS Wrote the main manuscript text and prepared figures. All authors read and approved the final manuscript.

## Acknowledgements

This research was funded by Warsaw University of Technology grant CyberiADa-1.

## References

- [1] Bionano Genomics. Bionano Genomics website. <https://bionanogenomics.com/>. Accessed 30 Sep 2021.
- [2] C. elegans Sequencing Consortium. Genome sequence of the nematode *C. elegans*: a platform for investigating biology, 12 1998.

- [3] J. Farlow, M. Nozadze, N. Mitaishvili, A. Kotorashvili, N. Kotoria, K. Arobelidze, V. Tavadze, T. Simsive, P. Imnadze, N. Latif, M. P. Nikolich, M. Washington, M. K. Hinkle, P. Kwon, and N. Trapaidze. Comparative genomic analysis of four multidrug-resistant isolates of *acinetobacter baumannii* from georgia, 2020.
- [4] J. L. Fierst. Using linkage maps to correct and scaffold de novo genome assemblies: methods, challenges, and computational tools. *Front Genet*, 6:220, 2015.
- [5] P. L. Freddolino, S. Amini, and S. Tavazoie. Newly identified genetic variations in common *Escherichia coli* MG1655 stock cultures, 01 2012.
- [6] K. Howe and J. M. Wood. Using optical mapping data for the improvement of vertebrate genome assemblies. *GigaScience*, 2015.
- [7] intel. Automated Relational Knowledge Base. <https://ark.intel.com/content/www/us/en/ark/products/75792/intel-xeon-processor-e52637-v2-15m-cache-3-50-ghz.html>, 07 2013.
- [8] E. S. Lander and M. S. Waterman. Genomic mapping by fingerprinting random clones: a mathematical analysis. *Genomics*, 2(3):231–239, 1988.
- [9] A. K. Leung, T. P. Kwok, R. Wan, M. Xiao, P. Y. Kwok, K. Y. Yip, and T. F. Chan. OMBlast: alignment tool for optical mapping using a seed-and-extend approach. *Bioinformatics*, 33(3):311–319, 02 2017.
- [10] A. K.-Y. Leung, M. C.-J. Liu, L. Li, Y. Y.-Y. Lai, C. Chu, P.-Y. Kwok, P.-L. Ho, K. Y. Yip, and T.-F. Chan. OMMA enables population-scale analysis of complex genomic features and phylogenomic relationships from nanochannel-based optical maps, 07 2019.
- [11] L. Mendelowitz and M. Pop. Computational methods for optical mapping. *Gigascience*, 3(1):33, 2014.
- [12] L. M. Mendelowitz, D. C. Schwartz, and M. Pop. Maligner: a fast ordered restriction map aligner. *Bioinformatics*, 32(7):1016–1022, 04 2016.
- [13] M. D. Muggli, S. J. Puglisi, and C. Boucher. Kohdista: an efficient method to index and query possible Rmap alignments. *Algorithms Mol Biol*, 14:25, 2019.
- [14] K. Mukherjee, D. Washimkar, M. D. Muggli, L. Salmela, and C. Boucher. Error correcting optical mapping data. *Gigascience*, 7(6), 06 2018.
- [15] Nabsys. Nabsys website. <https://nabsys.com/>. Accessed 30 Sep 2021.
- [16] R. M. Nowak, J. P. Jastrzebski, W. Kusmirek, R. Salamatin, M. Rydzanicz, A. Sobczyk Kopciol, A. Sulima Celinska, L. Paukszto, K. G. Makowczenko, R. Ploski, V. V. Tkach, K. Basalaj, and D. Mlocicki. Hybrid *de novo* whole-genome assembly and annotation of the model tapeworm *Hymenolepis diminuta*. *Scientific Data*, 6:1 – 6, 2019. doi:10.1038/s41597-019-0311-3.

- [17] J. S. Oliver, A. Catalano, J. R. Davis, B. S. Grinberg, T. E. Hutchins, M. D. Kaiser, S. Nurnberg, J. M. Sage, L. Seward, G. Simelgor, et al. High-definition electronic genome maps from single molecule data. *BioRxiv*, page 139840, 2017.
- [18] M. C. Riley, B. C. Kirkup, J. D. Johnson, E. P. Lesho, and C. F. Ockenhouse. Rapid whole genome optical mapping of *Plasmodium falciparum*. *Malar J*, 10:252, Aug 2011.
- [19] L. Salmela, K. Mukherjee, S. J. Puglisi, M. D. Muggli, and C. Boucher. Fast and accurate correction of optical mapping data via spaced seeds. *Bioinformatics*, 36(3):682–689, 02 2020.
- [20] D. C. Schwartz, X. Li, L. I. Hernandez, S. P. Ramnarain, E. J. Huff, and Y. K. Wang. Ordered restriction maps of *Saccharomyces cerevisiae* chromosomes constructed by optical mapping. *Science*, 262(5130):110–114, 10 1993.
- [21] J. A. Udall and R. K. Dawe. Is It Ordered Correctly? Validating Genome Assemblies by Optical Mapping. *Plant Cell*, 30(1):7–14, 2018.
- [22] A. Valouev, L. Li, Y. C. Liu, D. C. Schwartz, Y. Yang, Y. Zhang, and M. S. Waterman. Alignment of optical maps. *J Comput Biol*, 13(2):442–462, 3 2006.
- [23] A. Valouev, D. C. Schwartz, S. Zhou, and M. S. Waterman. An algorithm for assembly of ordered restriction maps from single DNA molecules. *Proc. Natl. Acad. Sci. U.S.A.*, 103(43):15770–15775, 10 2006.
- [24] A. Valouev, Y. Zhang, D. C. Schwartz, and M. S. Waterman. Refinement of optical map assemblies. *Bioinformatics*, 22(10):1217–1224, 05 2006.
- [25] C. Vranken, J. Deen, L. Dirix, T. Stakenborg, W. Dehaen, V. Leen, J. Hofkens, and R. K. Neely. Super-resolution optical DNA Mapping via DNA methyltransferase-directed click chemistry. *Nucleic Acids Res.*, 42(7):e50, 4 2014.